Salt formation associated with sub-surface boiling and supercritical water

M. Hovland[a,*], H.G. Rueslåtten[b], H.K. Johnsen[c], B. Kvamme[d], T. Kuznetsova[d]

[a]*Statoil, N-4035 Stavanger, Norway*
[b]*Numerical Rocks, N-7041 Trondheim, Norway*
[c]*Statoil, R&D Department, N-7005 Trondheim, Norway*
[d]*Department of Physics and Technology, University of Bergen, N-5000 Bergen, Norway*

Abstract

Laboratory experiments have demonstrated that supercritical water has extremely low solubility for normal sea salts. This fact opens up the possibility for the precipitation of salt from seawater that circulates in faults and fractures close to a heat source in tectonically active basins (typically extensional pre-rifts and rift settings). Seawater attains supercritical conditions at depths exceeding 2800 m (corresponding to a pressure of 300 bars) and temperatures above 405 °C. Salts may also precipitate by the boiling of seawater in sub-surface or submarine settings. This is demonstrated by a simple laboratory experiment. The theoretical basis for the precipitation of salts from seawater attaining supercritical condition has been examined by molecular modelling. These processes of salt precipitation constitute a new approach to the geological understanding of salt deposits, and two regions are selected to examine whether salt may have deposited under such hydrothermal conditions today: the Atlantis II Deep in the Red Sea (marine setting), and Lake Asale, Dallol, Ethiopia (continental setting).
© 2006 Elsevier Ltd. All rights reserved.

Keywords: Salt precipitation; Sub-surface boiling; Supercritical out-salting; Atlantis II Deep; Lake Asale

1. Introduction

Solar evaporation of seawater has long been established as the main process for the formation of salt deposits; mainly halite (NaCl) and anhydrite (CaSO₄). There are, however, numerous paradoxes and unresolved problems associated with this model as discussed by Warren (1999), Wilson (2003, 2004) and Talbot (2004) that clearly illustrate a lack of fundamental data, especially from the deepest portions of the salt basins, to verify this evaporite hypothesis as the general model for salt formation. The following citation from the most recent and authoritative Geological Encyclopedia (Selley, 2005) also underlines this conundrum: "As the name suggests, it was once thought that evaporites formed exclusively from the drying out of enclosed marine basins. This required improbably large volumes of seawater to provide the resultant

evaporites. It is now realized that many evaporites actually form in sabkhas (Arabic for 'salt marsh') from the replacement of pre-existing rocks, principally carbonates, by circulating brines. Evaporites should thus more correctly be termed 'replacementites'". Selley (2005) avoids, however, suggesting a possible origin for the 'circulating brines'. This problem is addressed in the present work.

But, salt deposits of geological significance are also known to have formed by hydrothermal processes (Momenzadeh, 1990; Lowell and Germanovich, 1997; Warren, 1999). There are two basic thermal processes which have to be addressed in this context: (1) the precipitation of salt from seawater and brines which attain supercritical conditions; and (2) precipitation of salt by the boiling of saline water in a (sub-marine) buried setting. The natural domain for supercritical water on the Earth is deep in the sub-surface and inside deep-sea hot vents (Von Damm et al., 2002; Kawada et al., 2004), well hidden from direct observations. Thus, the only factual observations of

*Corresponding author. Tel.: +47 958 022 43; fax: +47 51 99 5670.
E-mail address: mhovland@statoil.com (M. Hovland).

salt precipitating from supercritical saline waters come from laboratory experiments with visual access.

Bischoff and Rosenbauer (1985, 1989) performed benchmark laboratory experiments on high pressure and high temperature seawater systems, throughout the 1980s. Their work was done 'blind', i.e., without visual access to the high-pressure cell they used. This is probably one of the reasons why they failed to notice that small solid salt particles precipitated as the salt solutions passed well above the critical point (CP) on the boiling curve. Even so, Bischoff and Pitzer (1989) managed to assemble a table and a graph showing where solid salts occur, based on a review of their own and earlier work on NaCl–H$_2$O systems.

During examination of the phase behaviour of synthetic brines below and above their CPs, Armellini (1993) in his thesis work, and Tester et al. (1993), were, for the first time, able to visually observe what they called 'shock crystallization' of NaCl and Na$_2$SO$_4$ through the sapphire windows of their pressure cell. These were, however, pure 'physical' experiments and the geological significance of their results was not addressed before very recently (Hovland et al., 2005, 2006a, b). Because supercritical water oxidation is currently a rapidly expanding 'green science', further laboratory experiments on salt precipitation and scale control are common. Results from these experiments and also knowledge from geothermal energy production (Hodes et al., 2004; Kawada et al., 2004) confirm the results of Tester et al. (1993) and Bodnar et al. (1985) and modified the early graph from Bischoff and Pitzer (1989). These results have been reviewed by Hodes et al. (2004), from whom we have adapted Fig. 1, which is a phase diagram for NaCl–H$_2$O at the pressure of 250 bar. Here it is clearly seen that solid salt occurs in the supercritical seawater at temperatures from about 430 °C to about 720 °C.

The CP for distilled water is 374.15 °C and 221.2 bars. Beyond this point, the physical and chemical properties of water change fundamentally (Bellissent-Funel, 2001). These changes are documented by experimental measurements of the dielectric constant, ionic dissociation constant, and Raman spectral emissions. The static dielectric constant of water is equal to 80 at 'normal' (ambient) conditions, but drops as low as 2 at 250 bars and 450 °C (Bodnar et al., 1985; Tester et al., 1993; Hodes et al., 2004). Similarly, the ionic dissociation constant falls from 10^{-14} to 10^{-23} under supercritical conditions. Furthermore, the Raman spectra of supercritical deuterated water show only small residual amounts of hydrogen bonding (Franck, 1976; Kohl et al., 1991). This means that supercritical water essentially acts as a non-polar fluid with solvation properties resembling those of low-polarity organic fluids. For this reason, supercritical water (within a certain temperature and pressure range) is able to dissolve organic liquids but unable to dissolve common sea salts (Tester et al., 1993; Hodes et al., 2004), results which have also been modelled by molecular modelling (Hovland et al., 2006a).

Supercritical conditions for seawater and brines occur at pressures and temperatures elevated from those of pure water, i.e., ~300 bar and 405 °C for normal seawater (Bischoff and Pitzer, 1989). This pressure corresponds to a seawater depth of about 2800 m (Fig. 2). As the world average ocean depth is more than 3000 m, there is a large potential for the formation of supercritical water in the deep oceans and the underlying
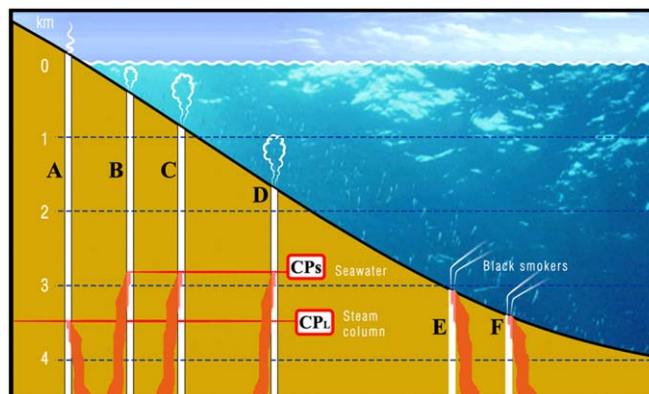
Fig. 2. An illustration of some supercritical and boiling environments on Earth, associated with terrestrial and oceanic hydrothermal systems. The column at the far left shows the association between boiling fresh water and depth, such as on Iceland, where the CP will be defined by a vapour (steam) column. The steam column forms above a deep-lying heat source (>374 °C) and the CP occurs deeper than 3 km, because the density of the steam column is low. However, in the ocean, beneath a cold seawater column, above a deep-lying heat source (>405 °C), the CP lies at around 2800 m (pressure of about 300 bar). The three middle vents have a CP lying at this depth, even though the seafloor depth varies. However, the two hot vents on the right have CPs at different depths, as they are both deeper than 2800 m and the CP is defined by temperature (cooling by seawater) rather than by depth. These 'black smokers' invariably construct sulphide and silicate chimney structures formed by mineral precipitation as supercritical fluids are instantly cooled by seawater. These chimneys actually contain and 'protect' (conserve) the migrating supercritical fluids.
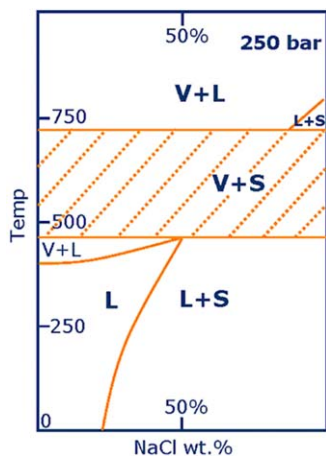

Fig. 1. This is a phase diagram for various salt concentrations and temperatures at a constant pressure of 250 bars. L is the Liquid, V the Vapour, S the Solid. Note that solid salts occur for temperatures up to 750 °C, depending on salinity. Note also that the envelope for S and V is from about 430–700 °C, this is the region we call 'supercritical out-salting'. Re-drawn from Hodes et al. (2004), and based on numerous publications, reviewed in Hodes et al. (2004).

water-saturated oceanic crust (Fig. 2), provided the presence of a heat source, i.e., intruding basalts with typical temperatures 800–1200 °C (Kawada et al., 2004).

Here, we present and discuss results from laboratory experiments and theoretical molecular modelling regarding the behaviour of seawater when heated to boiling in shallow water and under pressure to beyond the CP. Furthermore, these results and facts are discussed in terms of natural environments where analogue processes may occur, i.e., the Atlantis II Deep in the Red Sea and Lake Asale, Ethiopia. It is suggested that these processes are likely to occur several places on Earth, and that salt formation in hydrothermal settings may be of larger geological significance than hitherto realized.

2. A new model for hydrothermal salt formation

The new model for hydrothermal associated salt accumulations is based on five main prerequisites:

(1) a source of seawater or brine,
(2) a heat source of geological origin, i.e., a magma chamber ($T < 1200$ °C),
(3) a system of intersecting crustal faults and fractures above the heat source,
(4) a sedimentary unit located between (1) and (3) (which may be several kilometres thick),
(5) an environment that protects the salt from re-dissolving.

A sixth prerequisite is that the intervening sediments allow convection of fluids, i.e., that the pore-pressure is near hydrostatic from the surface down towards the heat-source along the 'flanking recharge zones', and slightly over-pressured along an upward 'central reflux zone' located above the heat-source (Fig. 3).

With these prerequisites satisfied, it is suggested that salts may precipitate in the following locations:

• at the terrestrial surface; from ascending saturated brines that evaporate in shallow ponds,
• at the bottom of deep confined ocean basins; by precipitation from ascending hot hyper-saline brines that cool in ponds on the seafloor,
• immediately above the heat-source; from out-salting under supercritical conditions within the central reflux zone,
• in the flanking recharge zone and the central reflux zone of the intervening sediments, at temperatures between 130 and 430 °C.

3. Solubility of salt in water—theoretical background

When salt is added to pure water, the system attains one more degree of freedom ('Gibbs phase rule') (Astarita, 1989; McCabe et al., 2001). Therefore, the onset of critical
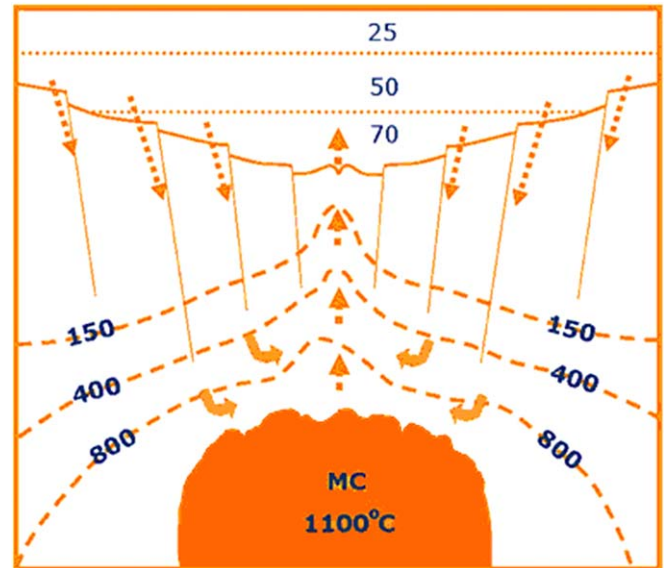

Fig. 3. A sketch (not to scale) illustrating our new conceptual geological model for the formation and accumulation of hydrothermally associated salts (see text). The sketch is drawn on the basis of inferred sub-surface conditions below the Atlantis II Deep, Red Sea (Ramboz et al., 1988; Zierenberg and Holland, 2004). Arrows indicate inferred movement of fluids and particles, including molten and precipitating salts, brines, salt slurry (mush) and other mineral particles and gases. MC is the magma chamber. The lines are inferred isotherms, in degrees C. The seafloor is at a general depth of 2100 m, and the magma chamber is inferred to be located at a depth of 1–1.5 km below seafloor. All temperatures are in C, also those shown in the water column.

behaviour will no longer occur at a single point, but along a curve that connects the CPs of the two pure components; salt and water. This is seen in T-p-X phase diagrams (Krauskopf, 1967; Palliser and McKibbin, 1997; Hodes et al., 2004) as two fluid phases that can coexist at any temperature, given the correct pressure and salt concentration. There is also a two-phase region on the T-p-X diagram (below 800 °C) with solid salt and supercritical vapour: 'the out-salting region'. Supercritical vapour in this region has extremely low solubility for salts, which means that most of the salts previously dissolved in the brine here exist in the solid phase. At temperatures below this out-salting region, but at pressures within, brine may exist in equilibrium with supercritical vapour (Fig. 4, based on Hodes et al., 2004).

The ability of water to dissolve salts is rooted in its highly dipolar nature which allows the water molecules to form spheres around the dissociated salt ions. These spheres of water will effectively screen the ion's charge (Debeye and Huckel, 1923) and significantly attenuate their Coulombic interactions with each other. The partial charges of the water molecules around the ions will orient themselves to minimize the deviations from average local electro-neutrality. This region is referred to as the solvent separated ion pair (SSIP) regime. As the temperature increases, the structure of the solution (i.e., the hydrogen-bonded network and clustering of water molecules around
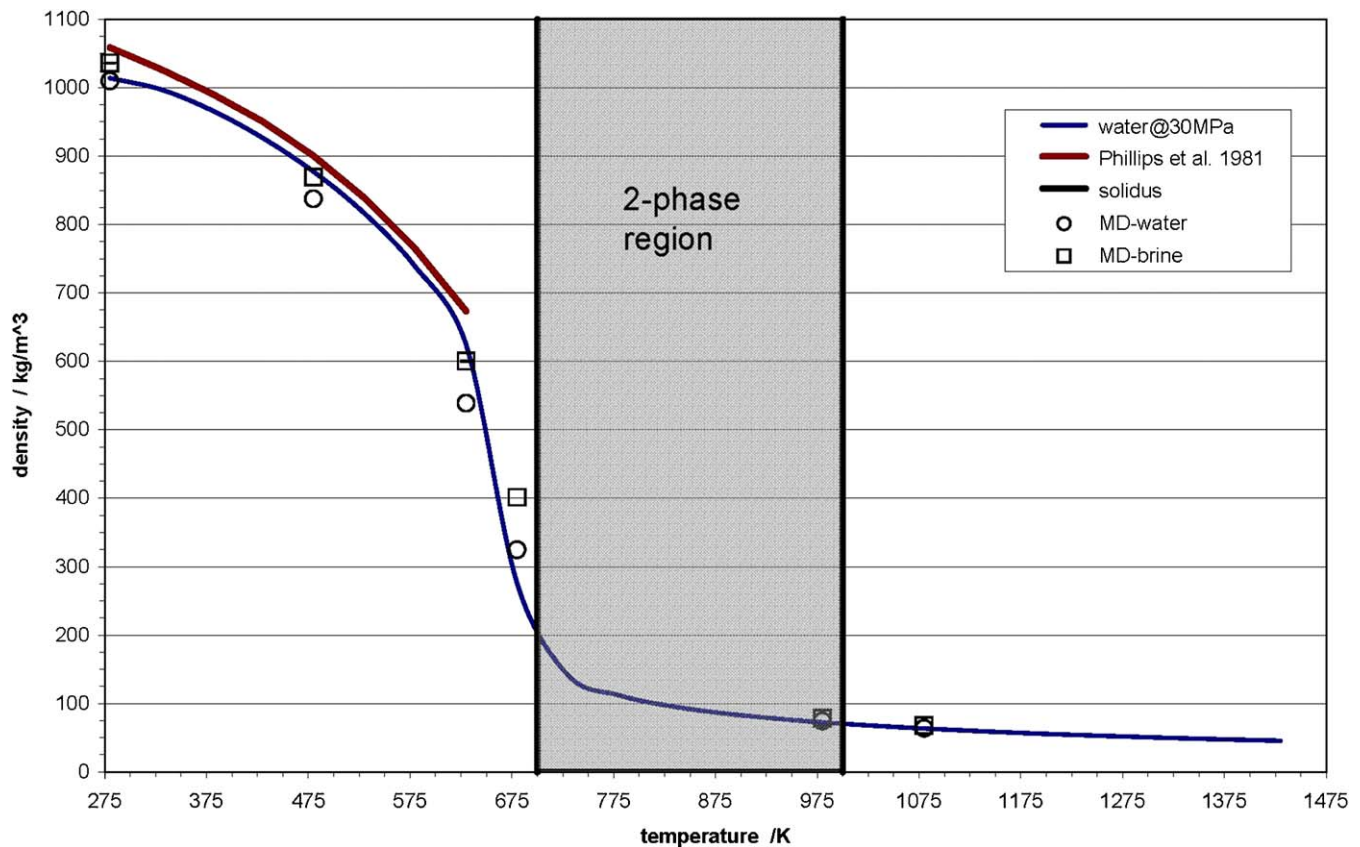
Fig. 4. The temperature dependence of water and brine density at a pressure of 300 bars. Red line is EoS data from Phillips et al. (1981); blue line is IAPWS-95 (Wagner and Preuss, 1995); circles are MD-simulated constant-pressure density results for pure water; squares, for 3.7% brine (seawater). The region between the two vertical lines is the 'out-salting range', where solid salts precipitate in supercritical water.

solutes) is gradually reduced. This is due to increasing the kinetic energy of the molecules and a concomitant reduction in the molecular interaction. The water dipole moment decreases faster with increasing temperature than the effective electrostatic force related to the ion charges. Consequently, the hydrogen-bonded network deteriorates and becomes unable to shield the salt ions effectively. This results in the precipitation of salt. In nature, this precipitation (and accumulation) of salts may take place in the subsurface when seawater passes through the CP-zone.

When the temperature is raised even higher, a regime will emerge where the ions are soluble again as electro-neutral ion pairs, surrounded by water molecules. This regime is called the contact ion pair (CIP) regime. Between the two regimes, SSIP and CIP, there is a two-phase equilibrium region where solid salt and supercritical vapour co-exist, i.e., the solid/fluid 'out-salting region' (Fig. 4). Here, the density of brine is plotted versus temperature (K) at 300 bar pressure, and the corresponding data from Phillips et al. (1981) are included.

The so-called pair-correlation functions describe the absence or presence of 'structures' in the solution for varying PT-conditions; i.e., the relative probability (with reference to ideal gas) of finding a given pair of atoms at a certain distance from each other. Pair correlation functions

can be derived from experimental studies of fluid structures (Soper, 1986; Soper and Phillips, 1986), estimated from statistical mechanical theories (Kvamme, 1995; Kvamme, 1997; Kvamme, 2002) or calculated from molecular simulations. The definition of a pair-correlation function is given by Eq. (1):

$$g_{\alpha_M\gamma_N}(r) = \exp\left\{-\beta\left[\varphi_{\alpha_M\gamma_N}(r) + \Delta\varphi_{\alpha_M\gamma_N}(r)\right]\right\}, \qquad (1)$$

where $g_{\alpha_M\gamma_N}(r)$ is the pair-correlation function between site α of molecule M and site γ of molecule N at a radial distance r. φ is the corresponding direct interaction energy and $\Delta\varphi$ the indirect interaction energy sampled through all possible intermediate interaction sites in the fluid. β is the inverse of the Boltzmann constant times temperature. Interactions between charges follow the Coulomb's law and diminish proportionally to the inverse distance. In addition to these long-range interaction energies, the molecules will have short-range repulsive and attractive interactions (van der Waals forces). The short-range attraction typically decays proportionally to the inverse of the radius to the sixth power. Similarly, the ions are characterized by their specific charges and short-range interactions. The inverse proportionality in temperature in Eq. (1) is the reason for the damping of the fluid structures and the corresponding changes in salt solubility with

increasing temperatures. The average number of water neighbours around a specific ion can also be estimated by integrating the pair correlation function. The oxygen atom dominates the water molecule and a good approximation of the number of water molecules, n_α, around a specific ion α can be found from Eq. (2) below

$$n_{\alpha\text{Oxygen}_\text{water}}(r_1, r_2) = 4\pi\rho_\text{water}\int_{r_1}^{r_2} g_{\alpha\text{Oxygen}_\text{water}}(r)r^2\,dr, \qquad (2)$$

where r_1 and r_2 are the range of radial distances from the centre of the ion α, i.e., integration from r_1 equal to zero, to r_2 corresponding to the first minimum of the pair correlation function, which will give the average number of water oxygen in the first coordination shell around the ion. Fig. 5(a) and (b) illustrate how the water structure changes, with temperature in a brine at 300 bars, according to the pair correlation functions.

4. Molecular simulations

The simulation model applied here (Nieto-Draghi et al., 2003; Guillot, 2002), describe atomistic-level interactions between water molecules in systems consisting of 512 water molecules and six molecules of NaCl, corresponding approximately to the normal seawater salinity of 3.5%. The SPC/E model was selected for describing the water–
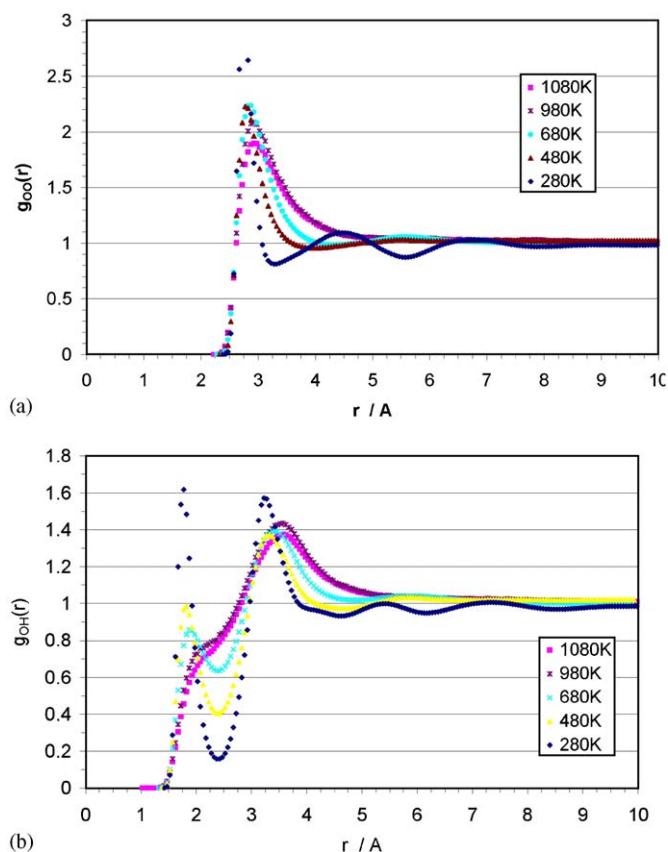

(a)

(b)

Fig. 5. Oxygen–oxygen (5a) and oxygen–hydrogen (5b) pair correlation functions in brine at pressure 300 bars and temperatures varying from sub- to supercritical (see text for further explanation).

water interactions in our simulations. The model by Smith and Dang (1994) was chosen for the ion descriptions. Cross-interactions were calculated using the Lorenz–Berthelot mixing rules (Allen and Tildesley, 1987).

Simulations were performed in a closed system at constant pressure and temperature. The thermostat parameters of the Nosé–Hoover formulation (Nosé, 1984; Hoover, 1989) were fixed at 100 femtoseconds (fs). The pressure control parameter was set to 8000 fs. For the rotational degrees of freedom we used an implicit quaternion scheme (Fincham, 1992), and the long-range electrostatic forces were handled using the Ewald summation approach (Allen and Tildeslay, 1987). Our simulated results are found to be in excellent agreement with previous numerical studies of similar systems (Lyubartsev and Laaksonen, 1996; Driesner et al., 1998; Chialvo and Simonson, 2003; Hodes et al., 2004).

An example of our numerical simulation results is given in Fig. 5 where the numerically simulated pair-correlations for oxygen and hydrogen in water are plotted as a function of temperature (K) at a pressure of 300 bars. The centre of mass in the water molecule is very close to the geometric centre of oxygen. In the absence of any preferences for the orientation of water molecules one would expect to find the first peaks of the oxygen–hydrogen pair-correlations at a separation close to the size of the oxygen atom. The fact that the first peak in the oxygen–hydrogen pair-correlation function lies closer than the corresponding peak in the oxygen–oxygen pair correlation function is evident for a hydrogen-bonded structure (preferential orientations of oxygen and hydrogen molecules in water). As the temperature increases, two phenomena emerge: firstly, there is a decrease in the height of the oxygen–hydrogen peak which is directly related to the strength of hydrogen-bonding. Secondly, there is a lack of any longer-range structures at high temperatures. This means that the hydrogen-bond network deteriorates and the water is essentially behaving as a non-polar fluid; loosing its ability to dissolve salts as ions (Fig. 5).

Fig. 6 describes the behaviour of the Na^+–Cl^- ion pair in terms of pair correlation functions at elevated temperatures below and above the two-phase limits. In particular, we should note the dramatic changes in the relative heights of the first (CIP) and second (SSIP) peaks of the Na^+–Cl^- correlation function. Supplementary evidence for the transition to a different solvation structure could be found in the oxygen–Na^+ and oxygen–Cl^- pair-correlation functions. One can find the average number of oxygen molecules surrounding each ion by integrating the pair-correlation function up to its first minimum and then multiplying by the average solution number density. The oxygen coordination numbers around the small Na^+ ions decreases almost linearly from 5.5 to 3.8, while the corresponding number for Cl^- ions increases from 7.3 to 12.3 for the same range of temperatures. From 980 K and upwards, the individual coordination numbers for both Na^+ and Cl^- decreases, as does the density of water.
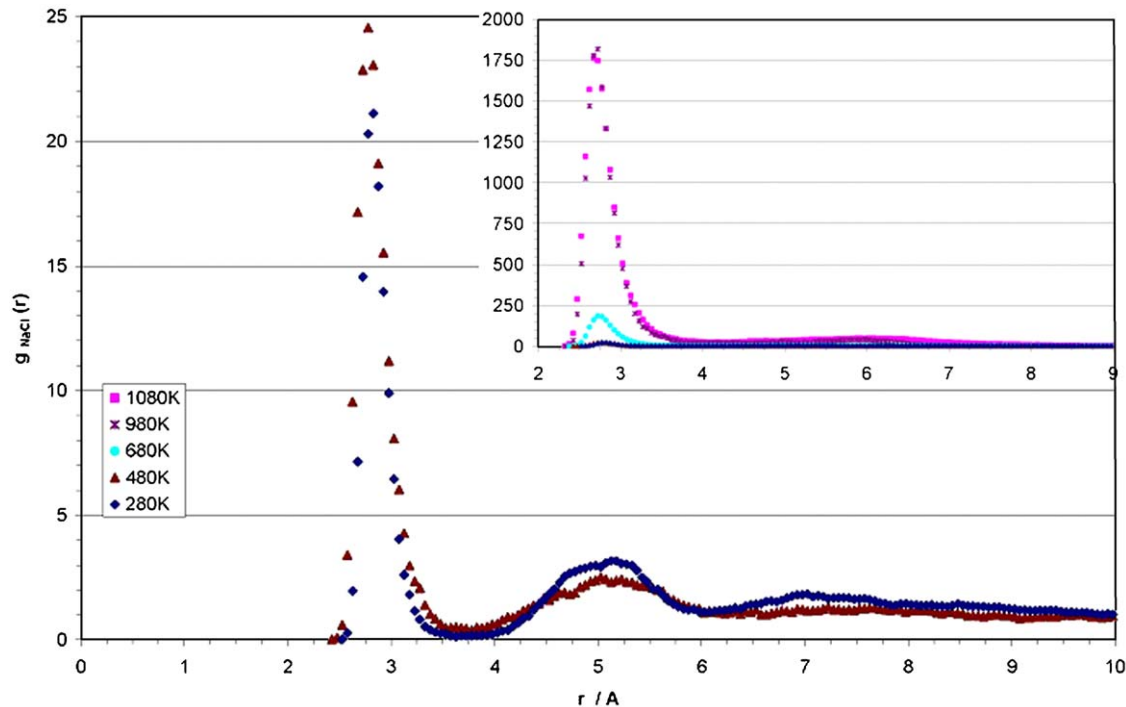
Fig. 6. Oxygen-chloride ion and oxygen-sodium ion pair correlation functions in brine at 300 bars for sub- and supercritical temperatures. Insert shows the higher temperatures (see text for further explanation).

5. Salt formation by boiling seawater

At ocean depths of less than 2800 m (i.e., pressures below 300 bars), seawater will not reach its CP and at sufficiently high temperatures it will boil, even when confined in sediments or in fractures of the crust. The boiling process can also produce large quantities of salts. Natural examples are: barite and anhydrite chimneys on the Piip submarine volcano offshore Kamchatka, Western Aleutians (Torokhov and Taran, 1994), and anhydrite mounds and chimneys near Grimsey island, off Northern Iceland (Hannington et al., 2001). It is well known that seawater easily becomes supersaturated with respect to anhydrite ($CaSO_4$) when heated beyond 130 °C (Bischoff and Seyfried, 1978). This happens because anhydrite has a retrograde solubility in water, i.e., it becomes less soluble with higher temperature.

In order to find out what actually happens in a submerged boiling seawater environment, a simple experiment was conducted. A 200 l steel tank containing 30 l of sand with an embedded heating element was placed on the bottom of a 7 m × 7 m concrete pool filled with seawater up to a depth of 3 m. The experiment was carried out as follows:

The open steel tank (50 cm diameter, 100 cm high) was equipped with a 5 kW heating element mounted horizontally 15 cm above the bottom of the tank (Fig. 7). The heating element consisted of three U-shaped tubes of 9 mm diameter and 48 cm length, and the sand (grain size: 0.6–1.4 mm) fully covered the heating element.

Two 8 mm holes were drilled in the bottom of the tank to allow seawater to circulate into the sand, and in order to ensure an upward flux of water (and steam), an inverted saucer-shaped steel plate was placed near the top of the sand surface, assuring a 5 mm clearance between this plate and the wall of the tank. This top lid was also fully covered with sand. Three temperature sensors were installed in the tank: one close to the heating element—used to control the heating effect, one under the inverted saucer plate, and one in the water column, 25 cm above the saucer plate. An automatic temperature switch turned off the heating element when the temperature close to the element attained 105 °C.

After 11 days of continuous boiling and monitoring, the tank was recovered and analyzed, and several conclusions could be made:

- After 3 days, the automatic temperature control reduced the heating element output by 50% (from 5 to 2.5 kW).
- The temperature measured at the heating element varied between 104 and 105 °C.
- The temperature in the water column above the saucer plate remained at a nearly constant temperature of 16 °C.
- On completion, an approximately 5 l volume, elongated artificial 'salt stock' had formed around the heating element (Fig. 7b, c).
- When the tank was removed from the pool, a 30 cm diameter white patch appeared on the concrete floor
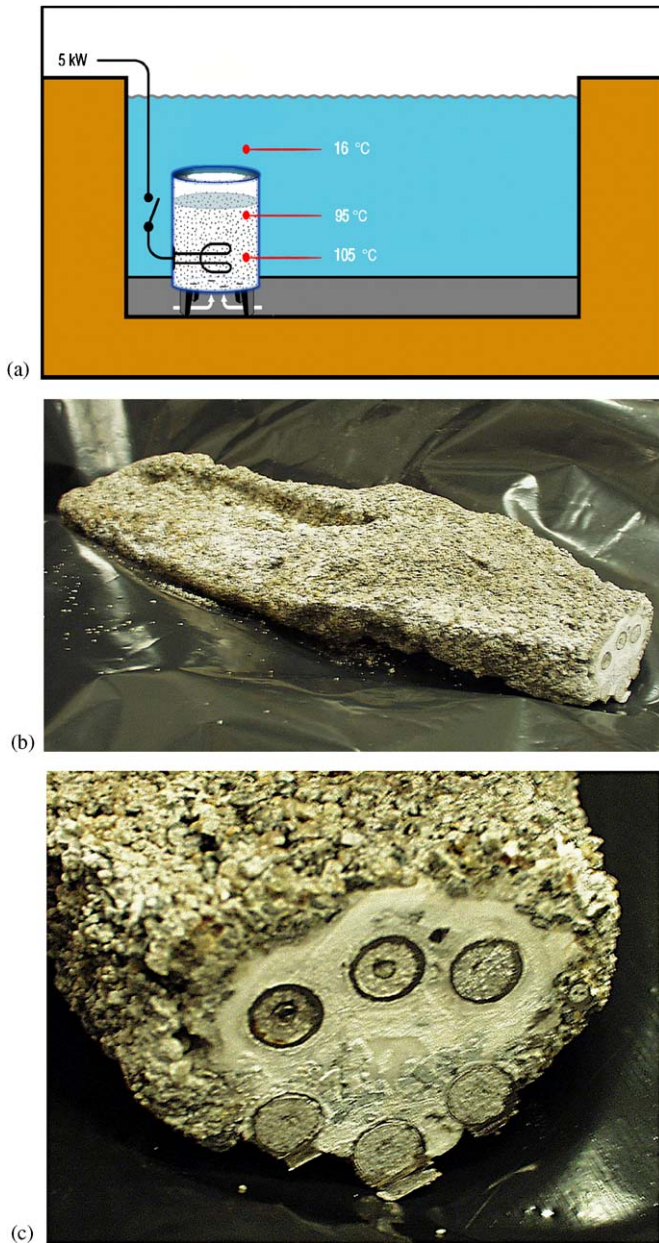
Fig. 7. (a) A sketch illustrating our submarine boiling experiment mentioned in the text, where a miniature artificial salt stock was formed. The sketch (not to scale) shows the experimental set-up for the submerged boiling of seawater inside a perforated steel tank. The apparatus was left for 11 days, with continuous submerged boiling. The steel tank contains sand through which the seawater circulated by convection. An automatic switch, set at a maximum temperature of 105 °C, was connected to the lowermost temperature sensor shown in the sketch. (b) The artificial miniature 'salt stock' produced in our experiment, by submerged boiling of seawater. Note the heating element, cut steel tubes far right. The 'salt stock' formed around the submerged heating element, which was buried in sand (see Fig. 7a). (c) A close-up photograph of the location where the three heating elements were cut off, and separated from the steel tank. Note that the sand has been pushed aside by the precipitated salts (displacive crystallization), mainly anhydrite with minor halite, which formed around the heating element (see Fig. 7a).

underneath the tank. ESEM (Environmental Scanning Electron Microscope) analysis showed it to consist of gypsum ($CaSO_4 \cdot 2H_2O$).

The subsequent investigations of the 'salt stock' included ESEM and XRD (X-ray Diffractometry) analyses. It was found that the miniature, artificial 'salt stock' consisted of anhydrite ($CaSO_4$) and small amounts of halite (NaCl) finely disseminated in the anhydrite phase. Some carbonate ($CaCO_3$) was also detected. The outer part of the salt stock consisted of sand cemented by salts.

Several important conclusions can be made from this simple experiment:

(1) When a sufficiently strong heat source is present, salts (dominated by anhydrite) precipitate in a porous (sandy) system, even when submerged in seawater.
(2) The salts precipitating closest to the heat source displace sand grains upon crystallization, and thus create a 'pure evaporite body'.
(3) The precipitation and crystallization process is relatively fast and will likely occur in the zone where circulating seawater makes contact with the available 'boiling surface'. This surface expands over time, in pace with the growing salt body.

This simple tank experiment indicates that the boiling of seawater can produce large quantities of salt over geological time scales, and the process may therefore represent an important geological process.

6. Case 1—The Red Sea, Atlantis II Deep

Up to 5 km thick deposits of bedded salts are found on the flanks of the central Red Sea (Lowell and Genik, 1972; Savoyat et al., 1989). These evaporites must have formed during the last 5 million years (Degens and Ross, 1969). In a study of the active hydrothermal processes of the Atlantis II Deep, Ramboz et al. (1988) found evidence of boiling brines and geyser-type discharges located at 2050 m water depth (Fig. 8). Liquid inclusions with up to ~33 wt% salts (NaCl equivalents) were also encountered: "Near-isothermal long-duration boiling of solutions implies a deep fluid reservoir with a limited volume, and heated by magma. The salt-enriched liquids were injected intermittently on the seafloor, then cooled without mixing" (Ramboz et al., 1988).

The Deep Sea Drilling Project (DSDP) Site 226 was located at 2169 m in the Atlantis II Deep. The purpose of the drilling was to sample the shallow basalt, but that was not achieved. Only a total of 14 m was penetrated, and two cores were obtained. These cores contained Late Quaternary sediments similar to those previously obtained from the area—a mixed montmorillonite, anhydrite, and goethite-hematite facies in the upper 5 m with fresh basalt fragments in the lower 9 m (Whitmarsh et al., 1974).

Furthermore, three pools of hot salty water are found within the Atlantis II Deep (Degens and Ross, 1969), and sediments underlying these brines are enriched in heavy
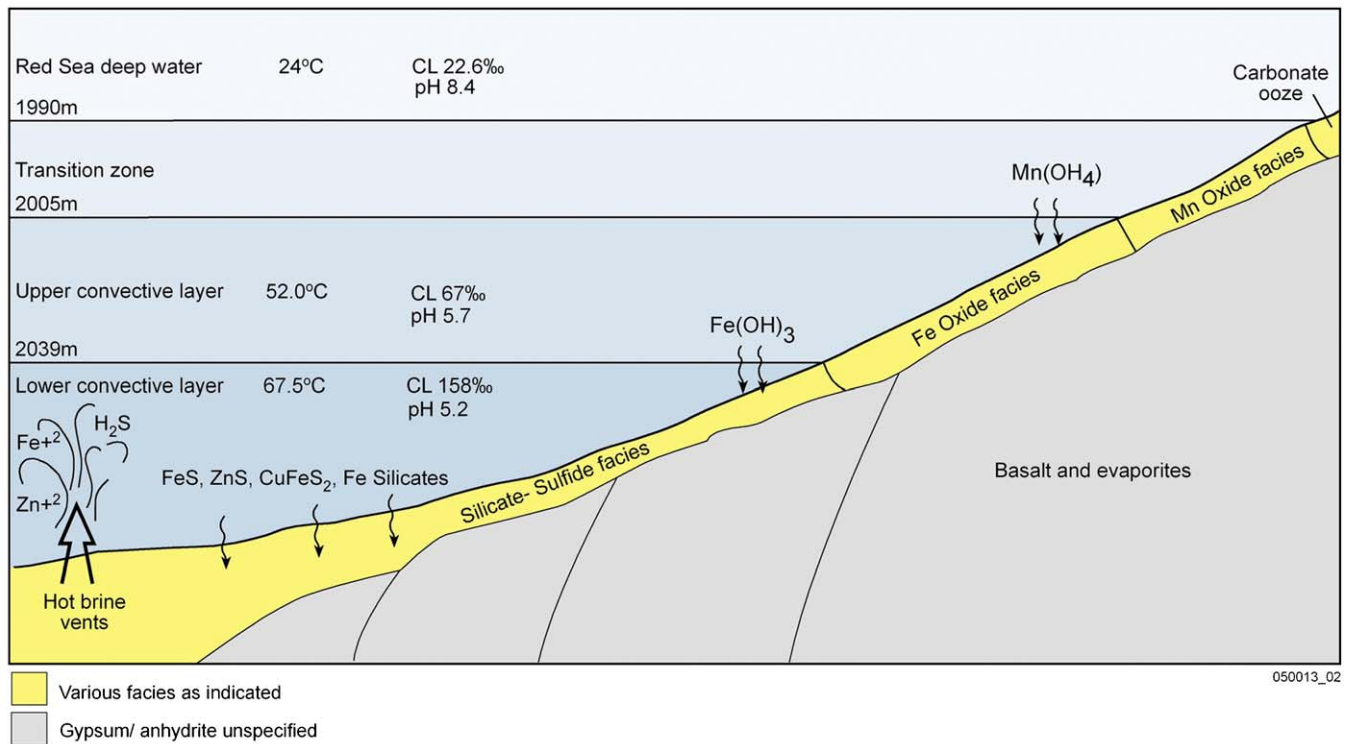
Fig. 8. The oceanographic and physical conditions in the Atlantis II Deep (not to scale), Red Sea, according to: Zierenberg and Holland (2004), Faber et al. (1998), Hartmann et al. (1998a, b), Zierenberg (1990), Danielsson et al. (1980). Note that hot brine 'fountains' occur in the Atlantis II Deep (Zierenberg and Holland, 2004).

metals (e.g. Cu, Pb, Zn, Ag, and Au). DSDP Site 225 was located 16 km to the east of the Atlantis II Deep, at 1228 m water depth. The drilling penetrated 230 m and terminated 54 m into the Late Miocene evaporite sequence. The deeper sedimentary units consist of anhydrite and halite interbedded with black shales (Orszag-Sperber et al., 1998). The dark muds and shales above the evaporite sequence are occasionally enriched with Fe, V (up to 1000 ppm), and Mo (up to 500 ppm). The black shale layers associated with the evaporite facies represent very finely laminated shales composed of clay, organic matter, and pyrite. The evaporite sequence is characterized by laminated to nodular anhydrite and halite.

The northernmost active hydrothermal systems in the Red Sea are the Kebrit and Shaban Deeps, located up to 500 km north of the Atlantis II Deep (Blum and Puchelt, 1991). According to Bonatti (1985), this part of the Red Sea consists predominantly of stretched and thinned continental crust: "Here, a few tectonically formed isolated deeps mark initial stages of sea-floor spreading with local emplacement of oceanic crust. Spreading rates are generally lower to the north, providing conditions for the precipitation of thick evaporite sequences, directly on oceanic crust (Girdler and Whitmarsh, 1974)." The poly-metallic massive sulphide deposits of the Kebrit and Shaban Deeps are sediment-hosted, with sediments abundant in gypsum (Blum and Puchelt, 1991).

7. The Atlantis II Deep in view of the new model

Extensive studies of buried hydrothermal systems, such as those conducted by the Ocean Drilling Program (ODP), have clearly demonstrated that seawater circulates deep into the sedimentary formations. For the Atlantis II Deep hydrothermal system, this means that seawater probably circulates right down to the magma chamber. This is despite the low-permeable intervening sediments. The DSDP drilling experience also clearly demonstrates that the sediments within the Atlantis II Deep are not 'normal' marine sediments, and that we are dealing with not only a hydrothermal salt producing system, but also a hydrothermal ore-forming system.

7.1. Zones of subaquatic salt formation

According to the new model, at least three zones of the Atlantis II Deep system possess the potential for salt formation:

1. In the warm brine pools on the seafloor, located at about 2100 m water depth (auto-precipitation due to cooling).
2. Within the central reflux zone (Fig. 3) above the magma chamber (supercritical conditions and boiling).
3. Within the flanking recharge zones (Fig. 3) (supercritical conditions and boiling).

The main driving force of the system is a strong local heat source, i.e., a magma chamber, which is inferred to have temperatures in the range 900–1200 °C. Its depth is unknown, but a depth of 1 km below seafloor is suggested (about 3 km below sea level) (Fig. 3), i.e., well within the supercritical window for circulating seawater.

7.2. Venting of brines and recharging

Observations of the Atlantis II Deep confirm the existence of some 'fountains' occurring on the seafloor immediately above the heat source (Fig. 8). In order to conserve mass, the emanating fluids from these fountains cannot continue to flow unless new fluids are drawn into the system. Consequently, there must be zones of recharge; although not directly observed. One recharge source may be the high-density brines located in the warm brine-pools on the sea bottom of the Atlantis II Deep. These heavy brines will likely sink down and flow along the flanks of the system and recharge the flow to the fountains. Portions of these sinking fluids may also mix with the upward-directed central flow feeding the 'fountains' (Figs. 3 and 8).

Within the flanking recharge zone the brines and seawater may attain a temperature of 130 °C at a relatively shallow depth beneath the sediment surface (Fig. 3). Here, the retrograde solubility of anhydrite will cause super-saturation, and anhydrite will precipitate. However, the brines will still contain many other dissolved (prograde) salts and this brine will continue to move deeper into warmer regions of the system. When the brines migrate deeper than 2800 m ($p = 300$ bar) and attain temperatures above 430 °C, they pass into supercritical condition and auto-precipitation of salts (mainly halite) will occur.

7.3. Temperatures associated with salt forming

The highest temperatures measured in the Atlantis II Deep brine-pools are in the range 60–70 °C. To account for the salt forming processes the various temperatures in the sediments/rocks above the magma chamber must be

- 130 °C (the temperature where anhydrite in seawater becomes supersaturated),
- 430 °C (the temperature where supercritical seawater precipitates NaCl at pressures above 300 bars),
- 800 °C (the melting point for halite).

7.4. Permeability of salt deposits

A sketch showing the inferred temperature zonations between the seabed and magma chamber is shown in Fig. 3. According to Lewis and Holness (1996) salt at depths of more than 3 km may have permeabilities similar to those of sandstones. Consequently, supersaturated brines will easily be transported through salt formations at these depths.

When the brine cools, salt particles are likely to re-crystallize.

7.5. Migration of water, brines and salt particles

At the zone closest to the magma-chamber, temperatures will be beyond 800 °C which is the melting point of most salts. Any molten salt that migrates out of this zone will come in contact with—and get mixed with supercritical water. This fluid will rise vertically in the central reflux zone, and the flux will be highest immediately above the magma chamber due to the buoyancy forces. When this fluid is cooled down during migration, it becomes super-saturated and salt particles form in the fluid and disperse.

At shallower depths than 2800 m (pressures below 300 bar), or at temperatures lower than 430–374 °C, the brines and fluids are sub-critical and boiling may occur. Boiling combined with upward flow induces cooling and condensation. Even if boiling does not occur, the phase change from supercritical vapour to sub-critical involves condensation from vapour to liquid. Condensation produces latent heat and pure water, which will dissolve the surrounding salts. However, it is envisaged that this warm and low-density, pure water will move fast, and may even reach the seafloor without affecting much salt (in a 'fountain' conduit). The inference is that some of this pure water may escape up to the sea surface and evaporate there.

7.6. Salt forming on the seafloor

Finally, salt may form within the brine-pools on the seafloor, fed by the brine venting fountains (Schreiber, 1988). When warm and high-density brines enter these pools, they start cooling, and many of the common sea salts (e.g. halite) will precipitate and accumulate on the seafloor.

The 'mother salt' below the Atlantis II Deep is reported to contain remnants of aligned halite chevron textures, which are primary sub-aqueous textures. This also points in the direction of salt formation in submarine brine pools. According to Warren (pers. com., 2005) these halites will re-crystallize into bi-axially compressed halokinetic textures; a set of textures clearly different from hydrothermal salt precipitates found in fractures and layers beneath the brine-filled pools of the Atlantis II Deep. This interpretation is also in agreement with that of Orszag-Sperber et al. (1998): "Evaporites deposited within an active rift system may be characterized by sub-aquatic facies because the irregular, structurally controlled coastal high relief areas preclude the development of sabkha-type evaporites."

8. Case 2—Lake Asale, Ethiopia

Thick layers of salts are deposited in Lake Asale, Danakil, Ethiopia. This location lies in the onshore triple-junction of a continental rift zone adjacent to the

Red Sea. Near Dallol of Lake Asale, seismic investigations indicate a salt thickness of at least 2200 m and a complicated internal structure with reflecting interfaces dipping in opposite directions at different levels (Talbot, 1978). Hot brine springs with temperatures well above 100 °C are venting on at least two of the dome structures.

The Dallol and Black Mountain areas bear clear evidence of igneous activity, as described by Holwerda and Hutchinson (1968): "Abundant direct evidence of igneous activity includes active volcanic peaks south of Lake Asale, basalts intercalated with evaporite beds east of the salt pan, recent cinder cones in the same area, the phreatic explosion at Black mountain, the volcanic cone at Mt. Maraho and the various circular, crater-like, features at Dallol, Horseshoe and Black mountains. The positive gravity and magnetic anomalies within the salt basin are indirect evidence of intrusions at depth."

Hochstein and Browne (2000) also commented on the Dallol 'salt volcanoes': "At Dallol (Danakil Depression) meteoric water enters a salt dome by advection and dissolves salt almost to the limit of NaCl solubility. The hyper-saline brine is heated by conduction from a cooling intrusion. This produces hot hyper-saline brine pools ($T = 110\,°C$); the TDS of the brine can be up to 420 g/kg, high in Na, K, Mg, and Cl. Here an overflow of hot brine causes the formation of salt mounds."

Perhaps the most intriguing aspects of the Asale salt deposits are the abundance of potash-bearing evaporites (KCl) and the venting of hot magnesium brines. Holwerda and Hutchinson (1968) commented upon this latter aspect: "Sometime after primary deposition, $MgCl_2$ was selectively leached from carnallite in the upper parts of the carnallite-rich zone to form the uppermost Sylvite member. This transformation may be taking place somewhere in the sub-surface due to igneous intrusions into the evaporites, which would account for the continually flowing, $MgCl_2$-saturated surface hot spring."

9. Lake Asale in view of the new model

The Dallol—Asale—Black Mountains area of the Danakil half-graben can be characterized as a large and complex geological 'salt factory'. Here, we will focus on the Dallol area where at least three salt volcanoes are active (Talbot, 1978) (Figs. 9 and 10). Hot brines are venting in the 'salt volcanoes' and deposit their brines and solid materials on the crater rims, on their slopes and on the surrounding salt flats where they form thick, near-horizontal evaporite layers.

9.1. Driving forces behind brine venting

The hot hyper-saline springs in Dallol can be interpreted as surface manifestations of local sub-surface heat-sources. Given that the total thickness of the evaporites at Dallol is 2.2 km, it is suggested that the heat sources that are driving the springs must be in the order of 1 km deeper; i.e., at
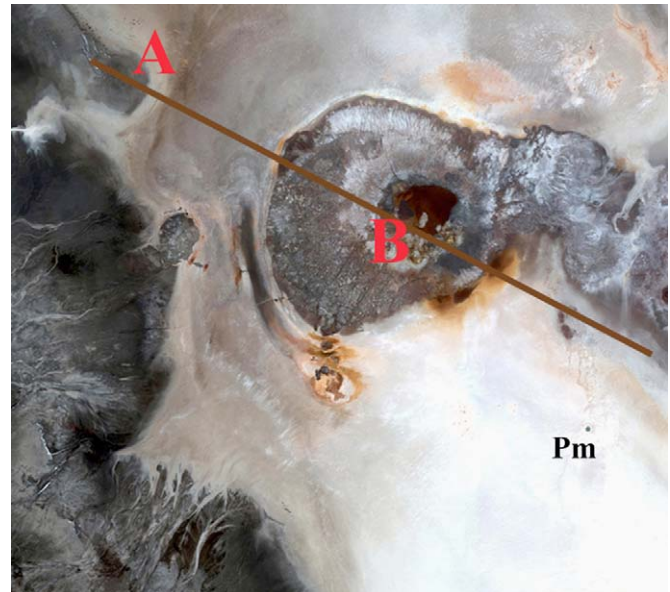

Fig. 9. A satellite image showing parts of Lake Asale. including the location of the seismic profile (straight line) acquired by Talbot (1978). Two 'salt volcanoes' are indicated (A and B). Boiling water and thick salt (halite) deposits are known to occur in these 'volcanic' craters. Hot brines flow from these craters and onto the surrounding pan, precipitating layered salts. Pm denotes 'pockmarks', circular crater features on the saltpan, resembling pockmarks found on the seafloor. They are suspected to be a result of seepage of (warm) brines to the surface.
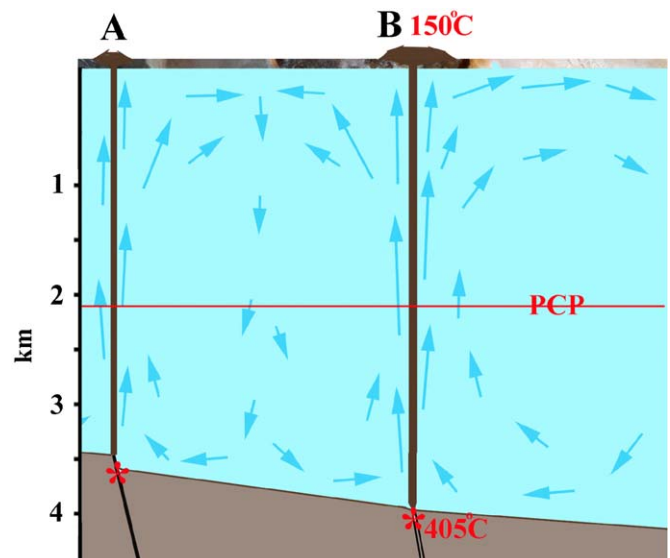

Fig. 10. An interpreted geoprofile through Lake Asale (not to scale), based on Talbot (1978), and on our supercritical out-salting model. 'A' and 'B' indicate the 'salt volcanoes' shown in Fig. 9. Blue arrows are inferred heatflow and convection patterns (mainly for liquid water and heat) through the salt lake (and solid salt). However, according to the seismic line shot by Talbot (1978), there is seismic structure in these deposits indicating convection as shown here. The red asterisks indicate where we expect supercritical water to exist, and where masses of solid salt are inferred to be deposited sub-surface, from the passage of brines into the supercritical domain.

3.2 km depth. If the temperatures of these heat-sources are higher than 405 °C there will be conditions for seawater/brines to attain supercritical conditions, and at temperatures above some 430 °C (depending on pressure) salt may precipitate and accumulate at these depths (as described for the Atlantis II situation).

Again, we have to address the conservation of mass for the venting liquids in the salt volcanoes. It is suggested that the high-density brines found in Lake Asale (Holwerda and Hutchinson, 1968) will circulate near to the heat sources and recharge the hydrothermal system (Fig. 10). In our interpretative model of the Lake Asale system, it is inferred that the region close to the individual heat-sources (at some 3.2 km depth) are characterized by intersecting faults and fracture systems. This rock volume may also contain hot injection sills. Realistic temperatures in this region may be in the order 400–600 °C, which means that the temperatures in the intervening volume between the surface volcanoes and the heat sources span from supercritical conditions at depth to boiling temperatures at depths shallower than 2.8 km.

9.2. Refining of salt

Salt production will, in large, follow the same pattern as that described for the Atlantis II Deep. Anhydrite will precipitate in the recharge zones, while halite and other salts precipitate in the supercritical zone nearer to the heat sources. Salt will also precipitate at the surface by solar evaporation in shallow pools (Schreiber, 1988). In order to account for the anomalous high-magnesium salts that precipitate, we theorize this to be a result of 'seawater starvation'. Because the Lake Asale region is cut off from the sea, there is likely very little new seawater being drawn into the system. The circulating water will preferentially leach the most soluble salts, thus 'refining' the primary salt. This preferential leaching of potassium and magnesium is a manifestation of processes that causes the "Potassium dilemma", i.e., the under-representation of potassium and magnesium in common rock salt compared to the composition of seawater. Furthermore, the leaching process may lead to deformations of the layered salt formations of Lake Asale (due to undermining). The salts of higher solubility that are preferentially drained out of the system are e.g. potash salts (KCl), magnesium salts (MgCl$_2$), and even iron-salts (FeCl$_2$) (Holwerda and Hutchinson, 1968). This process strongly indicates that parts of the layered salt sequences of Lake Asale are still undergoing deformation.

9.3. A hypothetic future formation of salt stocks

If this basin should, at some time in the geological future become buried by clastic sediments, it is easy to imagine that the 'salt volcanoes' may still produce exhalative hot brines and gases which will migrate upwards through vertical conduits in the newly deposited sediments and eventually form salt stocks.

10. Discussion

The processes discussed herein have very much in common with the processes governing the formation of submarine mineral chimneys and layered ore deposits. The necessary prerequisite conditions for such structures and deposits are

- long-lived sub-surface heat sources; associated with an
- extensive fault and fracture system; and
- hydrothermal circulation of water and brines.

The main problem, however, when it comes to regarding salt as just another ore-mineral, is its normally high solubility in water. The precipitated salts in sub-marine environments need protection against re-dissolution in the seawater.

10.1. Protection of precipitated salts

It is envisaged that tectonically active environments with high sedimentation rates may offer the best protection of sub-marine precipitated salts, due to fast sediment capping of the salt. Such protective environments may be found in rift zones, along transforms and transpression zones (e.g. the Dead Sea, the Red Sea, and parts of the Zagros salt belt). Also subduction zones and settings (e.g. under the Mediterranean Ridge; Westbrook and Reston, 2002) may offer protective environments for salt accumulations.

The Red Sea (our Case 1) is unique in that it is characterized by a relatively high sedimentation rate and is located near tropical climatic conditions, which secure a high surface evaporation. The surface evaporation will likely compensate for the venting of 'fresh' condensation water from sub-surface boiling and condensation from supercritical vapours. It can here be appropriate to note that condensation (fresh) water may easily be mistaken as meteoric water in various geological and hydrological settings. Thus, the migration of condensation water may explain not only the low-salinity formation waters encountered in some oil reservoirs (invariably interpreted as 'meteoric water'), but also non-saline, slightly acidic (pH ∼6) water found in shallow hot hydrothermal vents, such as the arsenic-charged hot vents off Ambitle Island, Papua New Guinea (Pichler et al., 2006).

Another interesting tectonic setting with a modern accumulation of salt is Lake Asale in Ethiopia (our Case 2), which is a terrestrial hydrothermal setting where the salt is protected by a warm and dry tropical climate. This will also secure rapid evaporation of the ascending brines. Hypersaline ponds on the seafloor are also environments for salt precipitation as described and discussed by Schreiber (1988). These ponds constitute a protective

environment for the brines from being diluted by seawater due to their high densities and stagnant water.

10.2. Permeability of salt deposits

Previously, salt formations have been treated as a near-impermeable medium to brines and hydrocarbons. However, contrary to this notion, Lewis and Holness (1996) provide results from deep drilling in buried salt bodies that point to considerable water–halite interaction. Furthermore, theoretical work by Holness (pers. com., 2005; Holness and Lewis, 1997) has resulted in the revelation that halite bodies at depths exceeding 3 km have permeabilities comparable to those of sandstones. Her work actually states that any free water in contact with salt at depths >3 km is preferentially 'sucked' into the salt structure in order for the system to reduce its internal free energy (same concept as discussed by Watson, 1982 for magmas). This opens up new realms for the composition of circulating basinal brines. Furthermore, this circulation of salt brines may also influence on sediments at shallower depths if the salt forms piercement structures such as diapirs (Holness, pers. com., 2005).

10.3. Accumulation and transport of solid salt

The amount of salts that will precipitate and accumulate in the zones of supercritical water conditions depend on the circulating volumes of seawater or brines, the volume of the fracture system and the longevity of the energy source; i.e. the size of the heat source. However, if available fracture volume is limited, the salts will likely be flushed upwards as concentrated brine/solid salt slurry together with supercritical gaseous water and condensation water. If the intervening rocks are thin, these fluids may exit onto the seafloor before passing through the CP and form white or black smokers (Von Damm et al., 2002).

10.4. Origin of hydrothermal fluids and salts

One of the main questions regarding the Lake Asale setting is from where the fluids originate. It is self-evident that meteoric water is participating in the processes of the system, but 'juvenile deep brines' of magmatic origin may also contribute (Sozansky, 2002; Kopf, 2002). Fluxes of magmatic water to volcanic lakes, such as those of Ruapehu (New Zealand) and Kelut (Indonesia) are estimated by Delmelle and Bernard (2000) to 7800 m^3 per day at Ruapehu and 2200 m^3 per day at Kelut. Also Degens and Kulbicki (1973) have observed emanations of brines and metalliferous hydrothermal solutions in Lake Magadi and Lake Kivu, West African Rift. Here, the centre of present day activity is at Lake Kivu, and sediments from the last 15,000 years carry distinct chemical 'fingerprints' of hydrothermal formation of stratiform ore deposits. They also conclude that the hydrothermal solutions are meteoric waters, which have derived their

metal and salt load by circulating through the volcanic rocks. The action of volcanic CO_2 and its supercritical component is also very important in these leaching processes.

Gases that are identified emanating from degassing magmas are H_2O, CO_2, SO_2, H_2S, HF, and HCl (Delmelle and Bernard, 2000; Chiodini et al., 2001), whereas water in contact with hot alkaline magmatic rocks become enriched in Na and Ca. Thus, all the chemical components necessary to form the common sea salts (halite, anhydrite, and carbonates) are present in the fluids from magmatic sources along the plate boundaries.

The model is also in accordance with the observation of high-temperature hydrothermal brines in terrestrial volcanic systems. Thus, at vent FC2 of Vesuvio volcanic crater, Italy, Chiodini et al. (2001) have found evidence for supercritical water and halite saturation. The pressures beneath this vent are estimated to be 260–480 bars, where there also occurs a subsurface reservoir of NaCl brines estimated to be close to halite saturation (49.2–52.5 wt% NaCl).

11. Summary and conclusions

This paper summarizes a study of salt forming processes of geological significance. The primary intention has been to improve the understanding of some basic processes associated with natural hydrothermal systems whereby sea salts (mainly halite and anhydrite) are precipitated and accumulated. The three main processes are

(1) Precipitation of salts from seawater and brines which attain 'out-salting conditions' in the supercritical zone of the sub-surface.
(2) Precipitation of salts by boiling of seawater or brines in the sub-surface; followed by
(3) Re-dissolution of salts by hot circulating (condensation) water and upward transportation towards the seafloor or the terrestrial surface.

Additional processes of importance are:

- Precipitation of anhydrite in regions where seawater attains temperatures above $\sim130\,°C$.
- Precipitation of halite upon cooling in warm pools with saturated brines located on the seafloor.

The laboratory and modelling experiments include the following:

- Laboratory observations and molecular modelling confirm that a spontaneous precipitation of salt occur when brines or seawater attain supercritical conditions. These conditions are attained in the sub-surface at >3 km depths (300 bars) and at temperatures above $430\,°C$.
- A simple laboratory experiment confirms that salts (anhydrite and halite) precipitate when seawater boils in

submerged porous sand, and that the salt is displacing the sand in contact with the heating element; thus forming a 'pure' salt body.

Based on published information from the Atlantis II Deep, Red Sea, and the Lake Asale area, Ethiopia, it is suggested that most of the salts deposited in these geological settings may have formed by the various modes of hydrothermally associated salt forming processes referred to above.

For salts produced in sub-marine settings, a relatively rapid sedimentation is favourable for protecting the salt from re-dissolution. Such environments are e.g. narrow and constricted rift basins. For terrestrial hydrothermally associated salt deposits, such as that of Lake Asale, a dry and warm climate is important so that any meteoric water rapidly re-evaporates, thus preventing excessive dissolution of the deposited salts. High-saline ponds on the seafloor (with precipitation of salts) are characterized by high-density and stagnant waters, which constitute a protective environment for the brine that otherwise would be diluted by seawater.

Acknowledgements

References

Allen, M.P., Tildesley, D.J., 1987. Computer Simulation of Liquids. Clarendon, Oxford, 410pp.

Armellini, F.J., 1993. Phase equilibria and precipitation phenomena of sodium chloride and sodium sulphate in sub- and supercritical water. Thesis. Massachussetts Institute of Technology, Cambridge, MA, USA.

Astarita, G., 1989. Thermodynamics: An Advanced Textbook for Chemical Engineers. Plenum Press, New York, 525pp.

Bellissent-Funel, M.-C., 2001. Structure of supercritical water. Journal Molecular Liquids 90, 313–322.

Bischoff, J.L., Pitzer, K.S., 1989. Liquid–vapor relations for the system NaCl–H_2O: summary of the P-T-X surface from 300° to 500 °C. American Journal of Science 289, 217–248.

Bischoff, J.L., Rosenbauer, R.J., 1985. An empirical equation of state for hydrothermal seawater (3.2% NaCl). American Journal of Science 285, 725–763.

Bischoff, J.L., Rosenbauer, R.J., 1989. Salinity variations in submarine hydrothermal systems by layered double-diffusive convection. Journal of Geology 97, 613–623.

Bischoff, J.L., Seyfried, W.E., 1978. Hydrothermal chemistry of seawater from 25 °C to 350 °C. American Journal of Science 278, 838–860.

Blum, N., Puchelt, H., 1991. Sedimentary-hosted polymetallic massive sulfide deposits of the Kebrit and Shaban Deeps, Red Sea. Mineralium Deposita 26, 217–227.

Bodnar, R.J., Burnham, C.W., Sterner, S.M., 1985. Synthetic fluid inclusions in natural quartz, III. Determination of phase equilibrium properties in the system H_2O–NaCl to 1000 °C and 1500 bars. Geochimica Et Cosmochimica Acta 49, 1861–1873.

Bonatti, E., 1985. Punctiform initiation of seafloor spreading in the Red Sea during transition from a continent to an oceanic rift. Nature 316, 33–37.

Chialvo, A.A., Simonson, J.M., 2003. Aqueous Na^+Cl^- pair association from liquid like to steam like densities along near critical isotherms. Journal of Chemical Physics 118 (17), 7921–7929.

Chiodini, G., Marini, L., Russo, M., 2001. Geochemical evidence for the existence of high-temperature hydrothermal brines at Vesuvio volcano, Italy. Geochimica Et. Cosmochimica Acta 65, 2129–2147.

Danielsson, L.G., Dryssen, D., Graneli, A., 1980. Chemical investigations of Atlantis II and Doscovery brines in the Red Sea. Geochimica Cosmochimica Acta 44, 2051–2065.

Debeye, P., Huckel, E., 1923. Zur Theorie der Elektrolyte, I, Gifrierpunktsniedrigung une verwandte Erscheinungen. Physikalische Zeitschrift 24, 185–206.

Degens, E.T., Kulbicki, G., 1973. Hydrothermal origin of metals in some East African rift lakes. Mineralium Deposita 8, 388–404.

Degens, E.T., Ross, D.A. (Eds.), 1969. Hot Brines and Recent Heavy Metal Deposits in the Red Sea. Springer, New York pp. 535–541.

Delmelle, P., Bernard, A., 2000. Volcanic lakes. In: Bjørnsson, B. (Ed.), Encyclopedia of Volcanoes. Academic Press, New York, pp. 877–895.

Driesner, T., Seward, T.M., Tironi, I.G., 1998. Molecular dynamics simulation study of ionic hydration and ion association in dilute and 1 molal aqueous sodium chloride solutions from ambient to supercritical conditions. Geochimica Et Cosmochimica Acta 62 (18), 3095–3107.

Faber, E., Botz, R., Poggenburg, J., Scmidt, M., Stoffers, P., Hartmann, M., 1998. Methane in Red Sea brines. Organic Geochemistry 29, 363–379.

Fincham, D., 1992. Leapfrog rotational algorithms. Molecular Simulation 8, 165–178.

Franck, E.U., 1976. Properties of water. In: Jones, D. de G., Staehle, R.W. (Eds.) High Temperature, High Pressure Electrochemistry in Aqueous Solutions. National association of corrosion engineers. Houston, TX, pp. 109–116.

Girdler, R.W., Whitmarsh, R.B., 1974. Miocene evaporites in Red Sea cores, their relevance to the problem of the width and age of oceanic crust beneath the Red Sea. In: Whitmarsh, R.B., Weser, P.E., Ross, D.A. (Eds.), Initial reports of the Deep Sea Drilling Project, vol. 23. US Government Printing Office, Washington, pp. 913–921.

Guillot, B., 2002. A reappraisal of what we have learnt during three decades of computer simulations on water. Journal of Molecular Liquids 101 (1–3), 219–260.

Hannington, M., Herzig, P., Stoffers, P., Scholten, J., Botz, R., Garbe-Schönberg, D., Jonasson, I.R., Roest, W., The shipboard scientific party, 2001. First observations of high-temperature submarine hydrothermal vents and massive anhydrite deposits off the north coast of Iceland. Marine Geology 177, 199–220.

Hartmann, M., Scholten, J.C., Stoffers, P., Wehner, F., 1998a. Hydrographic structure of brine-filled deeps in the Red Sea—new results from the Shaban, Kebrit, Atlantis II, and Discovery Deep. Marine Geology 144, 311–330.

Hartmann, M., Scholten, J.C., Stoffers, P., 1998b. Hydrographic structure of brine-filled deeps in the Red Sea: correction of Atlantis II Deep temperatures. Marine Geology 144, 331–332.

Hochstein, M.P., Browne, P.R.L., 2000. Surface manifestations of geothermal systems with volcanic heat sources. In: Bjørnsson, B.

(Ed.), Encyclopedia of Volcanoes. Academic Press, New York, pp. 835–855.

Hodes, M., Griffiths, P., Smith, K.A., Hurst, W.S., Bowers, W.J., Sako, K., 2004. Salt solubility and deposition in high temperature and pressure aqueous solutions. AIChE Journal 50 (9), 2038–2049.

Holness, M.B., Lewis, S., 1997. The structure of halite-brine interface inferred from pressure and temperature variations of equilibrium dihedral angles in the halite-H_2O–CO_2 system. Geochimica Et Cosmochimica Acta 61 (4), 795–804.

Holwerda, J.G., Hutchinson, R.W., 1968. Potash-bearing evaporites in the Danakil area, Ethiopia. Economic Geology 63 (2), 124–150.

Hoover, W.G., 1989. Generalization of Noses isothermal molecular-dynamics—non-hamiltonian dynamics for the canonical ensemble. Physical Review, A 40, 2814–2815.

Hovland, M., MacDonald, I., Rueslåtten, H., Johnsen, H.K., Naehr, T., Bohrmann, G., 2005. Chapopote asphalt volcano may have been generated by supercritical water. EOS 86 (42), 397–402.

Hovland, M., Fichler, C., Rueslåtten, H., Johnsen, H.K., 2006a. Deep-rooted piercement structures in deep sedimentary basins—manifestations of supercritical water generation at depth? Journal of Geochemical Exploration 89, 157–160.

Hovland, M., Kutznetsova, T., Rueslåtten, H., Kvamme, B., Johnsen, H.K., Fladmark, G.E., Hebach, A., 2006b. Sub-surface precipitation of salts in supercritical seawater. Basin Research 18, 221–230.

Kawada, Y., Yoshida, S., Watabane, S., 2004. Numerical simulation of mid-ocean ridge hydrothermal circulation including the phase separation of seawater. Earth Planets Space 56 (2), 192–215.

Kohl, W., Lindner, H.A., Franck, E.U., 1991. Raman spectra of water to $400\,°C$ and 3000 bar. Berichte - Bunsengesellschaft für Physikalische Chemie 95 (12), 1586–1593.

Kopf, A.J., 2002. Significance of mud volcanism. Review of Geophysics 40, 2–28.

Krauskopf, K.B., 1967. Introduction to Geochemistry. McGraw-Hill, New York, 721pp.

Kvamme, B., 1995. Interaction site representation of polar mixtures and electrolyte solutions. International Journal of Thermophysics 16, 743–750.

Kvamme, B., 1997. Structure and thermodynamics of water/methanol and water/ethanol mixtures from integral equation theory and molecular dynamics simulations. Fluid Phase Equilibria 131, 1–20.

Kvamme, B., 2002. Thermodynamic properties and dielectric constants in water–methanol mixtures by integral equation theory and molecular dynamics simulations. Physical Chemistry Chemical Physics 4, 942–948.

Lewis, S., Holness, M., 1996. Equilibrium halite–H_2O dihedral angles: high rock-salt permeability in the shallow crust? Geology 24, 432–434.

Lowell, J.D., Genik, G.J., 1972. Sea-floor spreading and structural evolution of southern Red Sea. American Association of Petroleum Geologists Bulletin 56, 247–259.

Lowell, R.P., Germanovich, L.N., 1997. Evolution of a brine-saturated layer at the base of a ridge-crest hydrothermal system. Journal of Geophysical Research 102 (B5), 10,245–10,255.

Lyubartsev, A.P., Laaksonen, A., 1996. Concentration Effects in Aqueous NaCl Solutions. A Molecular Dynamics Simulation. Journal of Physical Chemistry 100, 16410–16418.

McCabe, W.L., Smith, J.C., Harriott, P., 2001. Unit Operations of Chemical Engineering, International Edition. McGraw-Hill, New York, p. 508.

Momenzadeh, M., 1990. Saline deposits and alkaline magmatism: a genetic model. Journal of Petroleum Geology 13 (3), 341–356.

Nieto-Draghi, C., Avalos, J.B., Rousseau, B., 2003. Dynamic and structural behavior of different rigid nonpolarizable models of water. Journal of Chemical Physics 118, 7954–7964.

Nosé, S., 1984. A molecular-dynamics method for simulations in the canonical ensemble. Molecular Physics 52, 255–268.

Orszag-Sperber, F., Harwood, G., Kendall, A., Purser, B.H., 1998. A review of the evaporites of the Red Sea-Gulf of Suez rift. In: Purser, B.H., Bosence, D.W.J. (Eds.), Sedimentation and Tectonics of Rift Basins: Red Sea-Gulf of Aden. Chapman & Hall, London, pp. 409–426.

Palliser, C., McKibbin, R., 1997. A model for deep geothermal brines, I: T-p-X state-space description. Transport in porous media 33, 65–80.

Phillips, S.L., Igbene, A., Fair, J.A. Ozbek, H., Tavana, M., 1981. A Technical Databook for Geothermal Energy Utilization. Lawrence Berkley Laboratory Report, 12810.

Pichler, T., Amend, J.P., Garey, J., Hallock, P., Hsia, N.P., Karlen, D.J., Meyer-Dombard, D.R., McCloskey, B.J., Price, R.E., 2006. A natural laboratory to study arsenic geobiocomplexity. EOS, Transactions, American Geophysical Union 87 (23), 221–225.

Ramboz, C., Oudin, E., Thisse, Y., 1988. Geyser-type discharge in Atlantis II Deep, Red Sea: evidence of boiling from fluid inclusions in epigenetic anhydrite. Canadian Mineralogist 26, 765–786.

Savoyat, E., Shiferaw, A., Balcha, T., 1989. Petroleum exploration in the Ethiopian Red Sea. Journal of Petroleum Geology 12, 187–204.

Schreiber, B.C., 1988. Subaqueous evaporite deposition. In: Schreiber, B.C. (Ed.), Evaporites and Hydrocarbons. Columbia University Press, New York, pp. 182–255.

Selley, R.C., 2005. Mineralogy and classification. In: Selley, R.C., Cocks, L.R.M., Plimer, I.R. (Eds.), Encyclopedia of Geology. Elsevier, Amsterdam, pp. 27–37.

Smith, D.E., Dang, L.X., 1994. Computer simulations of NaCl association in polarizable water. Journal of Chemical Physics 100 (5), 3757.

Sozansky, V.I., 2002. On the deep origin of the Messinian salt in the Mediterranean. Conference Proceedings (abstr.): American. Assoc. Petroleum Geologists, Ancient oil—new energy technical program, Cairo, 2002.

Soper, A.K., 1986. On the determination of the pair correlation function from liquid structure factor measurements. Chemical Physics 107, 61–74.

Soper, A.K., Phillips, M.G., 1986. A new determination of the structure of water at 25C. Chemical Physics 107, 47–60.

Talbot, C.J., 1978. Halokinesis and thermal convection. Nature 273, 739–741.

Talbot, C.J., 2004. Extentional evolution of the Gulf of Mexico Basin and the deposition of Tertiary evaporates—discussion. Journal of Petroleum Geology 27 (1), 101–104.

Tester, J., Holgate, H.R., Armellini, F.J., Webley, P.A., Killilea, W.R., Hong, G.T., Berner, H.E., 1993. Supercritical water oxidation technology. In: Emerging technologies in hazardous waste management III, American Chemical Society, pp. 35–76.

Torokhov, P.V., Taran, Y., 1994. Hydrothermal fields of the Piip submarine volcano, Komandorsky back-arc Basin: Chemistry and origin of vent mineralization and bubbling gas. Bulletin of the Geological Society Denmark 41, 55–64.

Von Damm, K.L., Lilley, M.D., Shanks III., W.C., Bockington, M., Bray, A.M., O'Grady, K.M., Olson, E., Graham, A., Proskurowski, G., the souepr science party, 2002. Extraordinary phase separation and segregation in vent fluids from the southern East Pacific Rise. Earth and Planetary Science Letters 6490, 1–4.

Wagner, W., Preuss, A., 2002. The IAPWS formulation 1995 for the thermodynamic properties of ordinary water substance for general and scientific use. Journal of Physics and Chemistry Ref. Data 31, 387–535.

Warren, J.K., 1999. Evaporites: Their Evolution and Economics. Blackwell Science, Oxford, 438pp.

Watson, E.B., 1982. Melt infiltration and magma evolution. Geology 10 (5), 236–240.

Westbrook, G.K., Reston, T.J., 2002. The accretionary complex of the Mediterranean Ridge: tectonics, fluid flow and the formation of brine lakes—an introduction to the special issue of Marine Geology. Marine Geology 186 pp. 1–8.

Whitmarsh, R.B., Weser, P.E., Ross, D.A., 1974. Initial reports of the Deep Sea Drilling Project, vol. 23. US Government Printing Office, Washington, pp. 821–847.

Wilson, H.H., 2003. Extentional evolution of the Gulf of Mexico Basin and the deposition of Tertiary evaporates—reply to discussion. Journal of Petroleum Geology 26 (4), 403–428.

Wilson, H.H., 2004. Extentional evolution of the Gulf of Mexico Basin and the deposition of Tertiary evaporates—reply to discussion. Journal of Petroleum Geology 27 (1), 105–110.

Zierenberg, R.A., 1990. Deposition of metalliferous sediment beneath a brine pool in the Atlantis II Deep, Red Sea. In: McMurray, G.R. (Ed.), Gorda Ridge: A seafloor spreading center in the United States Exclusive Economic Zone. Springer, New York, pp. 131–142.

Zierenberg, R.A., Holland, M.E., 2004. Sedimented ridges as a laboratory for exploring the subsurface biosphere. In: Wilcock, W.S.D., DeLong, E.F., Kelley, D.S., Baross, J.A., Cary, S.C. (Eds.), The Subseafloor Biosphere at Mid-Ocean Ridges. Geophysical monograph Ser, No. 144, American Geophys. Union, pp. 305–323.

Further reading

Butterfield, D.A., Jonasson, I.R., Massoth, G.J., Feely, R.A., Roe, K.K., Embley, R.E., Holden, J.F., McDuff, R.E., Lilley, M.D., Delaney, J.R., 1997. Seafloor eruptions and evolution of hydrothermal fluid chemistry. Philosophical Transactions of the Royal Society of London, A 355, 369–386.

Cochran, J.R., 2005, Northern Red Sea: Nucleation of an oceanic spreading center within a continental rift. Geochemistry Geophysics Geosystems, AGU, Q03006, doi:10.1029/2004GC000826.